

PAPER • OPEN ACCESS

Fluids with power-law repulsion: Hyperuniformity and energy fluctuations

To cite this article: H Diamant and E C Oğuz 2025 *J. Phys.: Condens. Matter* **37** 065101

View the [article online](#) for updates and enhancements.

You may also like

- [Hyperuniformity in Ashkin–Teller model](#)
Indranil Mukherjee and P K Mohanty

- [Non-equilibrium dynamic hyperuniform states](#)
Yusheng Lei and Ran Ni

- [Hyperuniformity in phase ordering: the roles of activity, noise, and non-constant mobility](#)
Filippo De Luca, Xiao Ma, Cesare Nardini et al.

Fluids with power-law repulsion: Hyperuniformity and energy fluctuations

H Diamant¹  and E C Oğuz^{2,3,*} 

¹ School of Chemistry and the Center for Physics and Chemistry of Living Systems, Tel Aviv University, Tel Aviv 6997801, Israel

² Key Laboratory of Soft Matter Physics, Institute of Physics, Chinese Academy of Sciences, Beijing 100190, People's Republic of China

³ Songshan Lake Materials Laboratory, Dongguan, Guangdong 523808, People's Republic of China

E-mail: ecoguz@iphy.ac.cn

Received 22 July 2024, revised 16 October 2024

Accepted for publication 11 November 2024

Published 28 November 2024



CrossMark

Abstract

We revisit the equilibrium statistical mechanics of a classical fluid of point-like particles with repulsive power-law pair interactions, focusing on density and energy fluctuations at finite temperature. Such long-range interactions, decaying with inter-particle distance r as $1/r^s$ in d dimensions, are known to fall into two qualitatively different categories. For $s < d$ ('strongly' long-range interactions) there are screening of correlations and suppression of large-wavelength density fluctuations (hyperuniformity). These effects eliminate density modes with arbitrarily large energy. For $s > d$ ('weakly' long-range interactions) screening and hyperuniformity do not occur. Using scaling arguments, variational analysis, and Monte Carlo simulations, we find another qualitative distinction. For $s \geq d/2$ the strong repulsion at short distances leads to enhanced small-wavelength density fluctuations, decorrelating particle positions. This prevents indefinitely negative entropy and large energy fluctuations. The distinct behaviors for $s \geq d/2$ and $s < d/2$ give rise to qualitatively different dependencies of the entropy, heat capacity, and energy fluctuations on temperature and density. We investigate the effect of introducing an upper cutoff distance in the pair-potential. The effect of the cutoff on energy fluctuations is strong for $s < d/2$ and negligible for $s \geq d/2$.

Keywords: hyperuniformity, entropy, fluctuations, Coulombic fluids, Riesz gas

1. Introduction

Various physical systems contain long-range interactions which decay algebraically with the distance between particles. These include, for example, coulombic and dipolar fluids,

plasmas, topological defects in solids and liquid crystals, inclusions in elastic media and membranes, and vortices in superfluids. The statistical physics of such systems has been extensively studied; see reviews with comprehensive literature in refs [1–3]. The long-range interactions lead to various distinctive behaviors and anomalies, such as screening of correlations [4–6], super-extensive thermodynamic potentials [7] and sub-extensive fluctuations [8–10], repulsion-stabilized (Wigner) crystallization [11, 12], and strong surface effects that raise issues concerning the thermodynamic limit [13, 14] and the equivalence of statistical ensembles [15–18].

One of the anomalies occurring for repulsive power-law potentials is the suppression of long-wavelength density

* Author to whom any correspondence should be addressed.



Original Content from this work may be used under the terms of the [Creative Commons Attribution 4.0 licence](https://creativecommons.org/licenses/by/4.0/). Any further distribution of this work must maintain attribution to the author(s) and the title of the work, journal citation and DOI.

fluctuations, or hyperuniformity [3, 19, 20], which is directly tied to the sub-extensive fluctuations of particle number [8–10]. If the pair-potential decays as $1/r^s$ with $s < d$ (d being the number of dimensions), then the structure factor of the corresponding fluid, $S(\mathbf{k})$, which normally reaches a constant at small wavevectors k , instead decays to zero as $S(\mathbf{k}) \sim k^\alpha$, $\alpha = d - s$. The wavevector below which this decay takes place defines a screening length, beyond which the density fluctuations are suppressed. In section 3 we describe the emergence of hyperuniformity and the screening length based on intuitive scaling arguments.

A large body of rigorous theoretical work has accumulated over the years concerning systems with power-law interactions [1–3, 21–25]. These studies address, for example, the stability of crystalline structures [26, 27], fluid-solid transitions [28], the screening phenomenon [4, 6], sum rules associated with density correlations [29, 30], and particle-number fluctuations [8–10]. The present work does not continue this line of studies. Our goal is to turn the spotlight toward a different distinctive behavior of these systems, which to our knowledge has not been recognized. The indefinitely strong repulsion at *short* inter-particle distances, for $s \geq d/2$, leads to anomalous suppression of small-wavelength (large- k) density correlations. Such small-scale features are usually associated with non-universal molecular details and assumed not to affect the qualitative thermodynamics for densities that are not too high. However, we find that in the case of a power-law repulsion with $s \geq d/2$ this decorrelation [31] qualitatively changes the fluid’s thermodynamics, namely, how its entropy, heat capacity, and energy fluctuations scale with temperature and density, even at high temperature or low density. The relevant small length scale, akin to the Bjerrum length in coulombic fluids [32], is independent of the molecular size and typically larger.

In section 2 we define the problem and its parameters and present its characteristic length scales. In section 3 we obtain some of the qualitative results that follow, based on a simple scaling analysis. Section 4 provides a variational analysis which yields the high-temperature structure factor and entropy. In section 5 we show that for $s \geq d/2$ the results of section 4 yield a divergent entropy. We correct this failure using an intrinsic upper cutoff for k , obtaining modified scaling laws for the entropy and energy fluctuations. Section 6 presents Monte Carlo simulations, which confirm the analytical predictions and explore the effect of cutting off the power-law potential at a finite, large inter-particle distance. Finally, in section 7, we discuss the results and their experimental relevance.

2. The system

We consider an equilibrium fluid of N point-like particles in d -dimensional volume V and at finite temperature (in energy units) T . The mean density is $\rho_0 = N/V$. The particles interact

via the repulsive pair-potential

$$v(\mathbf{r}) = \frac{v_0}{r^s}, \quad v_0 > 0, \quad s \geq 0. \quad (1)$$

This model is sometimes referred to as the repulsive Riesz gas [3]. For a 3D coulombic fluid $s = 1$. The d -dimensional Fourier transform of the pair-potential (properly regularized) is

$$\tilde{v}(\mathbf{k}) = \frac{bv_0}{k^{d-s}}, \quad (2)$$

where b is a known numerical prefactor which depends on d and s . For a 3D coulombic fluid $d - s = 2$ and $b = 4\pi$.

The model has two intrinsic lengths, the mean inter-particle distance, $\rho_0^{-1/d}$, and the distance below which the pair-interaction energy is larger than T , $\ell = (v_0/T)^{1/s}$. For a 3D coulombic fluid $\ell = v_0/T$ is known as the Bjerrum length [32]. The two lengths define high- and low-temperature (equivalently, dilute and concentrated) regimes, $\ell\rho_0^{1/d} \ll 1$ and $\ell\rho_0^{1/d} \gg 1$, respectively. Out of the two lengths emerges a screening length, $\lambda \sim \ell^{-s/(d-s)}\rho_0^{-1/(d-s)}$, as discussed below. For a 3D coulombic fluid $\lambda \sim (\ell\rho_0)^{-1/2}$ is the Debye screening length [32].

We are interested in details of the equilibrium two-point correlation function of density fluctuations, $\langle \rho(\mathbf{0})\rho(\mathbf{r}) \rangle$, or its Fourier transform, the structure factor,

$$S(\mathbf{k}) = \rho_0^{-1} \langle |\tilde{\rho}(\mathbf{k})|^2 \rangle, \quad (3)$$

and its effect on the fluid’s thermodynamics.

3. Scaling analysis

The fact that the potential (1) has no characteristic length scale allows for several key results to be obtained from simple scaling arguments.

First, in the case of normal density fluctuations, $S(\mathbf{k})$ tends to a positive constant at small k [33]. If this were the case for the potential (1) with $s < d$, the energy of small- k density modes, $\tilde{v}(\mathbf{k})S(\mathbf{k})$, would diverge in the limit $k \rightarrow 0$ as $k^{-(d-s)}$. Avoiding it requires hyperuniformity, i.e. the structure factor must tend to zero at small k as $S(\mathbf{k}) \sim k^\alpha$, $\alpha \geq d - s$.

To see in more detail how this is brought about, consider a region of size R in the fluid. The mean number of particles in the region is $\langle n \rangle \sim \rho_0 R^d$. If the number fluctuations inside the region are normal, the variance of the number of particles is $\langle (\delta n)^2 \rangle \sim \langle n \rangle \sim \rho_0 R^d$. The number fluctuation δn entails the energy $\langle |\delta u| \rangle \sim \langle (\delta n)^2 \rangle v(R) \sim \rho_0 v_0 R^{d-s}$. This energy is provided by the thermal bath, $\langle |\delta u| \rangle \sim T$, leading to

$$R = \lambda \sim \left(\frac{T}{\rho_0 v_0} \right)^{1/(d-s)}. \quad (4)$$

If $s < d$, normal density fluctuations over distances larger than λ require energy larger than T and are suppressed. Thus, if the

repulsive potential is sufficiently long-ranged, $s < d$, screening occurs — normal density fluctuations are confined to within a screening length λ , which gets smaller with increasing density or decreasing temperature. For $s > d$ equation (4) gives the more common case of a correlation length λ getting larger with increasing ρ_0 or decreasing T . In this case normal density fluctuations with energy less than T occur over large length scales $R > \lambda$, while for $R < \lambda$ fluctuations cost more than T due to the (short-range) interactions.

For $s < d$, beyond the screening length, density fluctuations are anomalously small; the fluid is hyperuniform [20]. Let us assume that the number fluctuation for $R > \lambda$ is $\langle(\delta n)^2\rangle \sim \rho_0^{\gamma/d} R^\gamma$ with $\gamma < d$. (The power of ρ_0 is dictated by units.) The number fluctuation cannot grow with R more slowly than the region's surface R^{d-1} [34], i.e. the fluid cannot be more uniform than a crystal. Hence, $\gamma \geq d - 1$. The energy associated with this number fluctuation is now $\langle|\delta u|\rangle \sim \langle(\delta n)^2\rangle v(R) \sim v_0 \rho_0^{\gamma/d} R^{\gamma-s}$. Since it scales with R with an exponent $\gamma - s < d - s$, this energy is smaller than the one of normal fluctuations. It cannot decrease with R because this would favor strong large-wavelength fluctuations and lead to instability. Hence, $\gamma \geq \max(d - 1, s)$. The number fluctuation will have the smallest energy cost allowed for $\gamma = s$. Thus $\gamma = s$ if $s \geq d - 1$, and $\gamma = d - 1$ if $s < d - 1$. At the same time, the number-fluctuation exponent γ is mathematically tied to the structure-factor exponent α describing the approach of $S(\mathbf{k})$ to zero at small k , $S(\mathbf{k}) \sim k^\alpha$. The relation is $\gamma = d - 1$ if $\alpha > 1$ and $\gamma = d - \alpha$ if $\alpha < 1$ [20]. (These two cases are referred to, respectively, as class-I and class-III hyperuniformity; the marginal case $\alpha = 1$ is termed class-II hyperuniformity [20]. These relations have also been generalized to include some aperiodic systems [35, 36].) From the last two results it follows that $\alpha = d - s$.

To sum up the results of the scaling analysis: (a) for $s < d$ there are screening and hyperuniformity, (b) in this case we have at large R or small k the following hyperuniformity features:

$$\langle(\delta n)^2\rangle \sim R^\gamma, \quad \gamma = \begin{cases} s, & s \geq d - 1 \\ d - 1, & s < d - 1 \end{cases} \quad (5)$$

$$S(\mathbf{k}) \sim k^\alpha, \alpha = d - s, \quad (6)$$

and (c) these features take place beyond the screening length λ given by equation (4).

4. Structure from variational principle

A given structure factor $S(\mathbf{k})$ contains a certain amount of information concerning the structural correlations in a system. This information, restricted to pair correlations, sets an upper bound for the system's entropy. The upper bound \bar{h}_{ex} for h_{ex} , the excess entropy per particle over that of uncorrelated particles ($S(\mathbf{k}) = 1$), was calculated in references

[37, 38] to be

$$h_{\text{ex}}[S(\mathbf{k})] \leq \bar{h}_{\text{ex}}[S(\mathbf{k})] = \frac{1}{2(2\pi)^d \rho_0} \int d\mathbf{k} [\ln S(\mathbf{k}) - S(\mathbf{k}) + 1]. \quad (7)$$

The mean interaction energy per particle can be written in terms of the structure factor as well,

$$\begin{aligned} u[S(\mathbf{k})] &= \frac{1}{2N} \int d\mathbf{r} d\mathbf{r}' v(\mathbf{r} - \mathbf{r}') \langle \rho(\mathbf{r}) \rho(\mathbf{r}') \rangle \\ &= \frac{1}{2(2\pi)^d} \int d\mathbf{k} \tilde{v}(\mathbf{k}) S(\mathbf{k}). \end{aligned} \quad (8)$$

For $s > 0$ this integral diverges, but the divergence is removed by subtracting from u a constant $\sim \int d\mathbf{k} \tilde{v}(\mathbf{k})$. While equation (8) has been utilized to construct ground states that are disordered and hyperuniform [39], we focus here on the high-temperature limit. Equations (7) and (8) give a lower bound for the excess free energy per particle,

$$f_{\text{ex}}[S(\mathbf{k})] = u - T h_{\text{ex}} \geq f_{\text{ex}}^-[S(\mathbf{k})] = u - T \bar{h}_{\text{ex}}. \quad (9)$$

Setting $\delta f_{\text{ex}}^- / \delta S(\mathbf{k}) = 0$ gives

$$S(\mathbf{k}) = \frac{1}{1 + (\rho_0/T) \tilde{v}(\mathbf{k})}. \quad (10)$$

Since $\delta^2 f_{\text{ex}}^- / \delta S(\mathbf{k}) \delta S(\mathbf{k}') \sim [1/S(\mathbf{k})^2] \delta(\mathbf{k} - \mathbf{k}') > 0$, the structure factor (10) is a minimizer of the lower bound f_{ex}^- .

Equation (10) coincides with a known result for the structure factor of a fluid in the high-temperature regime [33]. Thus the bound becomes tight in this limit. Specializing equation (10) to the potential of equation (2), we get

$$S(\mathbf{k}) = \frac{k^\alpha}{k^\alpha + \lambda^{-\alpha}}, \quad \lambda = \left(\frac{T}{b v_0 \rho_0} \right)^{1/\alpha}, \quad \alpha = d - s. \quad (11)$$

For a 3D coulombic fluid this gives the known structure factor with $\alpha = 2$ and the Debye screening length, $\lambda = [T/(4\pi v_0 \rho_0)]^{1/2}$ [33].

The results above agree with the scaling analysis, equations (4) and (6). Moreover, the limiting behavior of equation (11), $S(k \ll \lambda^{-1}) \sim k^\alpha$, is demanded by exact sum rules at all temperatures [29, 30]. Thus, although the equality $h_{\text{ex}} = \bar{h}_{\text{ex}}$ and the structure factor (11) are strictly valid only in the high-temperature limit, we expect them to be qualitatively applicable also away from this limit. This will be confirmed by simulations in section 6 for $s < d/2$. For $s \geq d/2$, the analyses given above fail, as discussed in the next section.

5. Entropy and energy fluctuations

Substituting $S(\mathbf{k})$ of equation (11) back in the integral of equation (7) gives an upper bound for the entropy, which

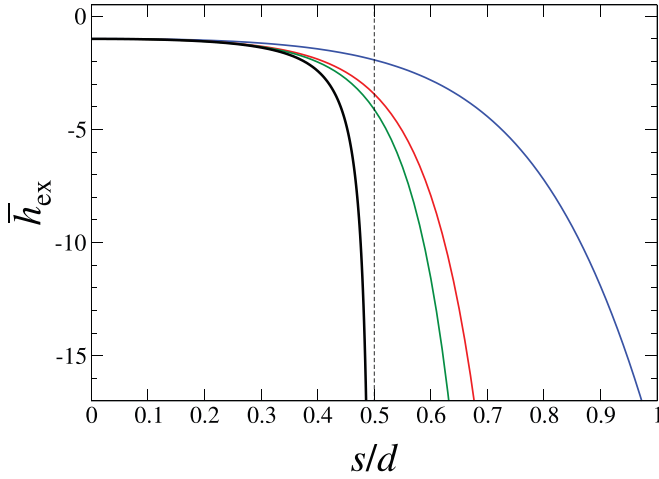


Figure 1. Upper bound on the entropy cost per particle due to density correlations, as a function of s/d . The entropy is rescaled by the prefactor given in equation (12). The lowest, black curve shows the function $\psi(s/d)$, giving the rescaled entropy bound for $s < d/2$ and diverging as $s/d \rightarrow 1/2$; see equation (12). From top to bottom, the blue, red, and green curves give the rescaled entropy bound as a function of s for $d=2$, according to equation (14), with the upper cutoff $\lambda K = 10, 50, 100$, respectively. As the cutoff increases the curves approach divergence at $s = 1$ (i.e. $s/d = 1/2$).

depends only on $\rho_0 \lambda^d$ and s/d . For $s/d < 1/2$, the result is

$$\bar{h}_{\text{ex}} = \frac{\mathcal{S}_d}{2(2\pi)^d d \rho_0 \lambda^d} \psi(s/d),$$

$$\psi(x) = \frac{\pi x}{1-x} \frac{1}{\sin[\pi/(1-x)]}, \quad s/d < 1/2, \quad (12)$$

where \mathcal{S}_d is the surface of the unit sphere in d dimensions. For a 3D coulombic fluid $\mathcal{S}_d = 4\pi$ and $\psi(1/3) = -1/6$, yielding $\bar{h}_{\text{ex}} = -(24\pi\rho_0\lambda^3)^{-1}$, which coincides with the entropy obtained from the Debye–Hückel theory. Thus the bound is equal indeed to the actual entropy in the high-temperature limit.

However, the situation is more subtle. The function $\psi(x)$ is shown by the lowest, black curve in figure 1. It tends to $-\infty$ as $x \rightarrow 1/2$, i.e. as s tends to $d/2$ from below. For $s \geq d/2$, $\bar{h}_{\text{ex}} \rightarrow -\infty$. Since \bar{h}_{ex} is an upper bound, this result implies that the entropy itself diverges.

The divergence indicates a failure of the high-temperature theory presented above. It comes from the large-wavevector limit of the integration in equation (7), i.e. not from the long range of the interaction but rather from the strong repulsion at small r . The larger the value of s , the stronger the interaction of nearby particles which, according to the theory above, would result in strongly correlated large- k density modes. If the approach of $S(\mathbf{k})$ to 1 at large k is not sufficiently fast, the negative contribution of these strong correlations to the entropy diverges. Introducing an upper cutoff K for $|\mathbf{k}|$ to

regularize this divergence, we readily find

$$\bar{h}_{\text{ex}} \sim \begin{cases} -K^{2s-d}, & d/2 < s < d \\ -\ln K, & s = d/2. \end{cases} \quad (13)$$

In more detail, the integration in equation (7) can be performed with the upper cutoff K , yielding

$$\bar{h}_{\text{ex}} = \frac{\mathcal{S}_d}{2(2\pi)^d d \rho_0} K^d [\ln S(K) + (1 - \alpha/d) {}_2F_1(1, d/\alpha; 1 + d/\alpha; -(\lambda K)^\alpha)] \quad (14)$$

$$\stackrel{\lambda K \gg 1}{\simeq} -\frac{\mathcal{S}_d}{4(2\pi)^d \rho_0 \lambda^d} \times \begin{cases} \frac{1}{2s-d} (\lambda K)^{2s-d}, & d/2 < s < d \\ \ln(\lambda K), & s = d/2, \end{cases} \quad (15)$$

where ${}_2F_1$ is the hypergeometric function. The results of equation (14) for $d=2$ and $\lambda K = 10, 50, 100$ are shown by the upper three curves in figure 1. As the cutoff is increased, the curves approach the divergent curve for infinite K .

The upper- k cutoff must affect various measurable quantities derived from the entropy. For example, assuming that the bound is tight, $h_{\text{ex}} \simeq \bar{h}_{\text{ex}}$, as expected at sufficiently high temperature, we obtain the excess heat capacity and mean square fluctuation of the potential energy per particle as

$$c_{\text{ex}} = T \frac{\partial \bar{h}_{\text{ex}}}{\partial T}, \quad \langle (\Delta u)^2 \rangle = T^2 c_{\text{ex}}. \quad (16)$$

For $s < d/2$ we get from equations (12) and (16) $\langle (\Delta u)^2 \rangle \sim T^2 \lambda^{-d} \sim T^{(d-2s)/(d-s)}$. (The anomaly for $s \in (d/2, d)$ is seen also here; for these values of s the energy fluctuations supposedly decrease rather than increase with temperature.)

The particles being point-like, a natural choice for the lower cutoff length is ℓ , the distance below which the pair-repulsion v_0/r^s is stronger than T ,

$$\ell = (v_0/T)^{1/s}, \quad K = c/\ell, \quad (17)$$

where c is an unknown numerical factor. Substituting this cutoff in equation (15) and using equation (16), we find

$$\text{high temperature: } \langle (\Delta u)^2 \rangle \sim \begin{cases} \rho_0^{s/(d-s)} T^{(d-2s)/(d-s)}, & s < d/2 \\ \rho_0 T^{(2s-d)/s}, & d/2 < s < d \\ \rho_0 \ln(T/\rho_0), & s = d/2. \end{cases} \quad (18)$$

The prefactors can readily be worked out from the equations above. Thus, the dependencies of the potential energy fluctuations on temperature and density are qualitatively different for $s < d/2$ and $s \geq d/2$. Equation (18) holds at sufficiently high temperature because it assumes that the cutoff K is sufficiently large, $\lambda K \sim T^{(d/s)/(d-s)} \gg 1$.

As ℓ does not represent a sharp barrier, K cannot be a sharp cutoff. For $s \geq d/2$ we expect the amplitudes of density modes with $k \gtrsim K$ to be finite but become less correlated than predicted by equation (10). Namely, $1 - S(k \gtrsim K)$ should decay faster than $(\lambda k)^{-\alpha}$. As the temperature is increased, $K \sim T^{1/s}$ increases, and the deviation of $S(\mathbf{k})$ from equation (10) should

occur at larger and larger wavevectors. At a sufficiently high temperature the cutoff will have to be replaced by a finite particle size, which is not included in the present theory.

As the temperature decreases, ℓ increases and the cutoff K decreases. If we conjecture that equation (14) should qualitatively hold also in the low-temperature (equivalently, high-density) regime, $\lambda K \ll 1$, we obtain $\langle (\Delta u)^2 \rangle \sim \rho_0^{-1} T^{d/s+2} \ln T$. This dependence on T is stronger than the high-temperature one given in equation (18), for both $s < d/2$ and $s \geq d/2$.

6. Simulations

We run swap Monte Carlo simulations of a two-dimensional system with N point-like particles, interacting via the truncated and shifted version of the pair-potential $v(\mathbf{r})$ of equation (1):

$$v_c(\mathbf{r}) = \begin{cases} \frac{v_0}{r^s} - \frac{v_0}{r_c^s} & \text{if } r \leq r_c, \\ 0 & \text{else,} \end{cases} \quad (19)$$

with an interaction-cutoff distance r_c of the order of the system size. The introduction of r_c has three motivations. (a) By exploring the effect of r_c on the results we address the complications associated with finite-size (boundary) effects in systems with long-range interactions [40, 41]. (b) Sensitivity of the results to the value of r_c indicates dominance of large-wavelength fluctuations. (c) Long-ranged interactions without a cutoff require the inclusion of a one-body potential (i.e. a neutralizing background as in the case of the one-component plasma model) to ensure stability [42, 43]. In the remainder of this section we derive the equations and present the results for $d = 2$.

We run 250 independent NVT simulations at each prescribed temperature by starting from different initial configurations. Each simulation runs for 2×10^5 Monte Carlo sweeps and is sampled every 5×10^2 sweeps where a sweep corresponds to an attempted move of each of the $N = 2000$ particles under periodic boundary conditions in a square box of side length L . The first 1×10^5 sweeps contain swaps between two randomly selected individual particles with a swap attempt probability $p = 0.3$ [44, 45], followed by further 1×10^5 sweeps with standard Metropolis algorithm without swapping. Our results are sampled from the latter part without swapping and averaged over the 250 runs. The step size for attempted moves is adjusted such that the acceptance rate is approximately 40%.

The simulations are performed for a low-density fluid with $\rho_0 = 0.002$ and at temperatures between $T/v_0 = 0.2$ and $T/v_0 = 200$, using a unit of length equal to $L/1000$. We study interaction potentials with $s = 0.5, 1.2, 1.5$ and $r_c = L/2, L/8$. Although we do not investigate the low-temperature behavior in detail in the present work, we observed the formation of a hexagonal crystal in our finite systems upon quenching down to absolute zero in a few test cases. In the studied temperature range we do not observe crystallization. Thus, the systems

considered have a crystalline ground state with a melting temperature lower than the lowest temperature studied here.

To compare our numerical results with the theory, we first provide an analytical expression for the structure factor with the interaction-cutoff distance r_c . The 2D Fourier transform of the truncated potential (19) for $s < 2$ reads as

$$\tilde{v}_c(\mathbf{k}) = 2\pi r_c^{2-s} v_0 \left(\frac{{}_1F_2\left(1 - s/2; 1, 2 - s/2; -(kr_c)^2/4\right)}{2 - s} - \frac{J_1(kr_c)}{kr_c} \right), \quad (20)$$

where J_1 is the Bessel function of the first kind, and ${}_1F_2$ denotes the hypergeometric function. Specializing the structure factor of equation (10) to the modified potential of equation (20) yields

$$S_c(\mathbf{k}) = \frac{1}{1 + 2\pi r_c^{2-s} (v_0/T) \rho_0 B(kr_c)}, \quad (21)$$

where the function $B(kr_c)$ is given as

$$B(kr_c) = \frac{{}_1F_2\left(1 - s/2; 1, 2 - s/2; -(kr_c)^2/4\right)}{2 - s} - \frac{J_1(kr_c)}{kr_c}. \quad (22)$$

In the large-wavelength limit $B(kr_c \ll 1) \simeq 1/(2 - s) - 1/2$. Consequently, the limit of $S_c(\mathbf{k})$ in equation (21) becomes

$$S_c(k \rightarrow 0) = \frac{1}{1 + \frac{\pi r_c^{2-s} s (v_0/T) \rho_0}{2 - s}}. \quad (23)$$

As $r_c \rightarrow \infty$ we recover the hyperuniformity, $S(k \rightarrow 0) \rightarrow 0$, for pure power-law potentials with $s < d$ (here $s < 2$). In the small-wavelength limit, we have $B(kr_c \gg 1) \sim (kr_c)^{-(2-s)}$, leading to $1 - S_c(\mathbf{k}) \sim (k\lambda)^{-(2-s)}$. We recall that for $s \geq d/2$ (here $s \geq 1$) this decay of the theoretical $1 - S_c(\mathbf{k})$ with increasing k is too slow to avoid the divergence of the entropy. Thus, no matter how short the potential cutoff r_c may be, the correlations at wavelengths smaller than $\min(r_c, \ell)$ must be suppressed to avoid the anomaly for $s \geq d/2$.

In figure 2 we show $S_c(k)$ as obtained from MC simulations (circles), together with the theoretical prediction given in equation (21) (full lines), for $s = 0.5, 1.2, 1.5$ (i.e. s both smaller and larger than $d/2 = 1$), using a cutoff distance $r_c = L/2$. In all panels the temperatures are in decreasing order from top to bottom, $T/v_0 = 100, 20, 10, 5, 2, 1, 0.5$. The insets demonstrate the effect of the interaction cutoff as obtained theoretically in equations (11) and (21). The structure factors $S(k)$ in the absence of a cutoff (dashed lines) decay to zero for $k \rightarrow 0$ as k^{2-s} . The structure factors $S_c(k)$ with a cutoff (solid lines) level off at sufficiently small k , reaching their limit value $S_c(k \rightarrow 0)$ given in equation (23).

As seen in figure 2, which is focused on small k , the simulation results and theoretical predictions agree remarkably well for small s and high temperature, including fine

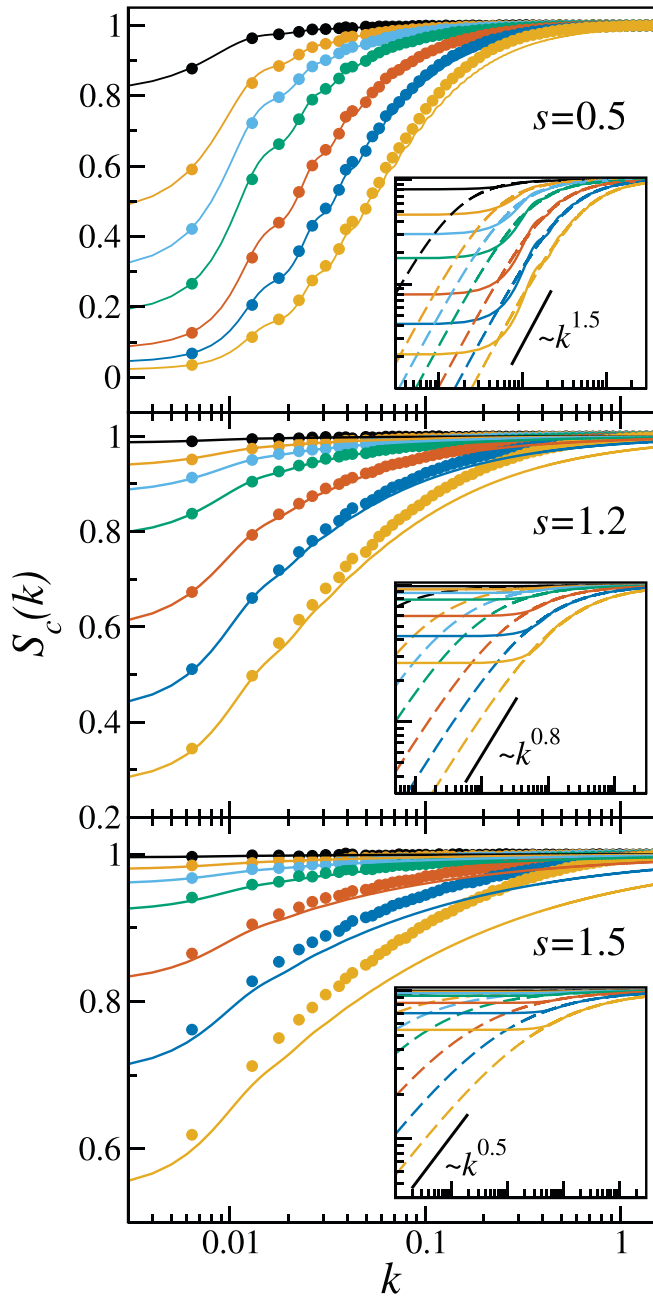


Figure 2. Structure factors obtained from MC simulations (circles) and from the variational analysis (equation (21), solid lines). The different data sets, from top to bottom, correspond to decreasing temperature, $T/v_0 = 100, 20, 10, 5, 2, 1, 0.5$. Upper, middle, and lower panels show the results for the interaction exponents $s = 0.5, 1.2, 1.5$, respectively (i.e. s both smaller and larger than $d/2$). The interaction cutoff is $r_c = L/2$. The unit of length is $L/1000$. The insets compare the theoretically predicted structure factors with interaction cutoff $r_c = L/2$, $S_c(k)$ (equation (21), full lines), with those for pure power-law repulsion without a cutoff, $S(k)$ (equation (11), dashed lines). The thick black lines in the insets indicate the scaling behavior of $S(k)$ in the small- k limit, $S(k) \sim k^{d-s}$ with $d = 2$.

oscillatory features in $S_c(k)$ (upper panel; see more below). For larger s and smaller T , the deviation of the theory from the simulation is larger and begins at a smaller value of k .

This is probably due to higher-order correlations, neglected by the theory, which should become less significant with increasing temperature and increasing range of interaction. Still, the simple high-temperature theory, which considers only two-point correlations, captures well the behavior at sufficiently small k even for the lower temperatures.

The structure factor $S_c(k)$ exhibits small oscillations (see the upper panel in figure 2). These oscillations are a result of the interaction cutoff distance r_c . They are absent in $S(k)$ for pure power-law potentials. The periodicity Δk of the oscillations corresponds to $2\pi/\Delta k \approx r_c$. As most studies on fluids focus on either short-ranged interactions or purely long-ranged interactions without a cutoff (using, e.g. Ewald sums), this oscillatory effect, to our best knowledge, has not been presented before. The fact that the oscillations are pronounced for $s = 0.5$ (upper panel) and negligible for $s = 1.2, 1.5$ (lower two panels) indicates the sensitivity of the longer-range interactions (small s) to the interaction cutoff.

In figure 3 we turn our attention to the large- k modes. To examine how the structure factor approaches 1 at large k we plot $1 - S_c(\mathbf{k})$ as obtained from MC simulations and from equation (21). As predicted in section 5, density fluctuations on this small scale (large k) are enhanced, decorrelating the density modes at these length scales. Thus the fluctuations of particle number become more quickly Poissonian with increasing k than what would be expected from the strong inter-particle repulsion. This is manifested in large deviations of $1 - S_c(k \gtrsim K)$ from the predictions of the high-temperature theory, equations (10) and (21). The deviations become stronger and sharper as s is increased and as the temperature is decreased, as anticipated. Figure 3 shows also the locations of the crossover wavevectors, $k \sim 1/\ell$, beyond which the decorrelation should occur (dashed vertical lines). The k values where the structure factor starts deviating from the theory are correlated with $1/\ell$, as conjectured; yet, for $s = 1.2, 1.5$ they are significantly smaller than $1/\ell$. This wider range of enhanced fluctuations expands the validity range of our main results as it implies that the enhancement occurs already for wavelengths much larger than the typical molecular size. The deviations for $s = 1.5$ are sharper than for $s = 1.2$ without an appreciable change in $1/\ell$, highlighting the effect of increasing s on the magnitude of enhancement in addition to its location. Deviations from the theory are present also for $s = 0.5 < d/2$, which has not been anticipated. They are much smaller and less sharp than for $s > d/2$ and begin at k values closer to $1/\ell$ (upper panel). Consequently, they do not have a significant effect on the thermodynamics, as we show next.

In section 5 we have predicted a qualitatively different dependence of the potential energy fluctuations on temperature for $s < d/2$ and $s \geq d/2$; see equation (18). In figure 4 we show numerical and analytical results for the fluctuations of the potential energy per particle $\langle (\Delta u)^2 \rangle$ as a function of T for $s = 0.5, 1.2, 1.5$. The analytical results are obtained using equations (14), (16), (17), and (21).

Comparing the uppermost panel of figure 4 with the lower two, we clearly see the qualitative differences between the two

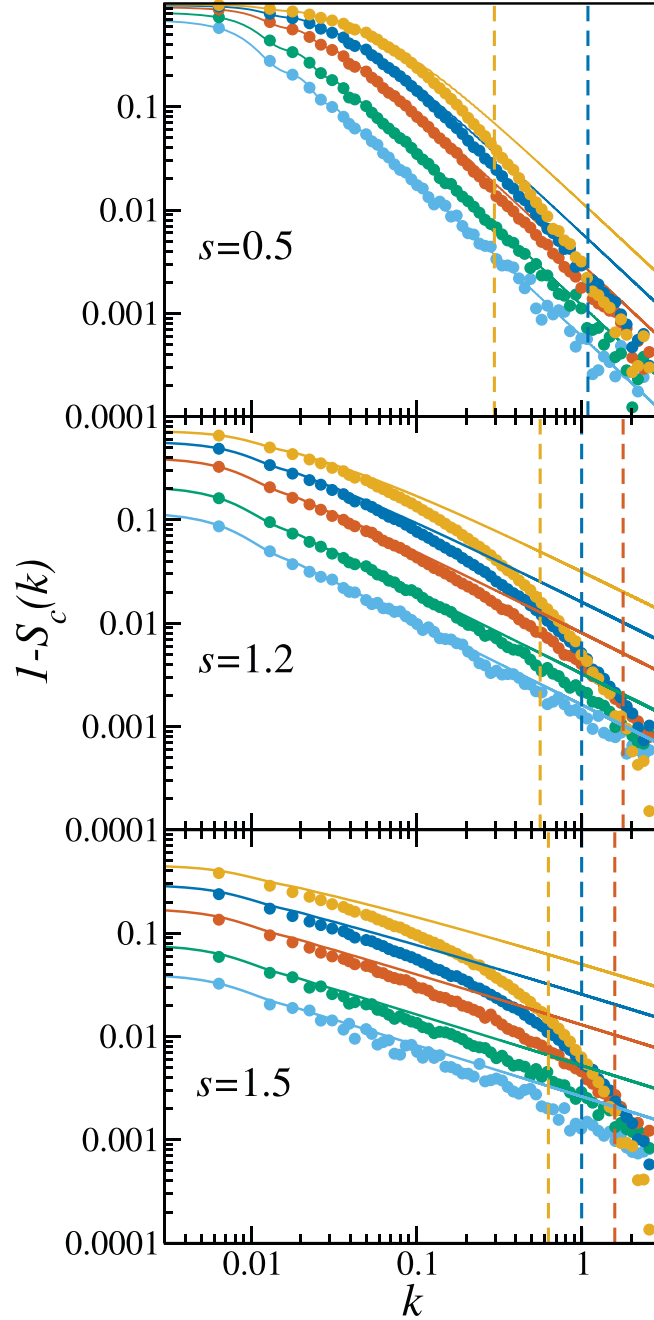


Figure 3. Approach of the structure factor to 1, $1 - S_c(k)$, from MC simulations (circles) and theory (equation (21), solid lines). The three panels show results for $s = 0.5, 1.2, 1.5$. The temperature are, from top to bottom, $T/v_0 = 0.5, 1, 2, 5, 10$, with color coding as in figure 2. The vertical dashed lines indicate the wavevectors $k = 1/\ell$ (equation (17)) for $T/v_0 = 0.5, 2, 5$ (left to right).

categories. First, the data follow the different power laws predicted at high temperature (equation (18)), $(d - 2s)/(d - s) = 2/3$ for $s = 0.5$, and $(2s - d)/s = 1/3, 2/3$, for $s = 1.2, 1.5$, respectively. In addition, we find a very different effect of the interaction cutoff distance r_c on the energy fluctuations. For $s = 0.5$ the cutoff distance makes the fluctuations saturate to a constant value at high temperature. (Recall that the fluctuations are of the potential energy only.) The constant value increases with r_c , as it should assuming that the

saturation disappears in the limit of infinite r_c . The crossover between the power law and the saturation occurs around the temperature for which $\lambda(T) = r_c$ (see the dashed vertical lines). Above that temperature the screening length exceeds the interaction cutoff distance, leaving no room for long-range effects such as hyperuniformity. In other words, when $\lambda(T) > r_c$ the interaction is essentially short-ranged. Thus the sensitivity to r_c indicates the dominant contribution of large-wavelength fluctuations for $s = 0.5 < d/2$. By contrast, the

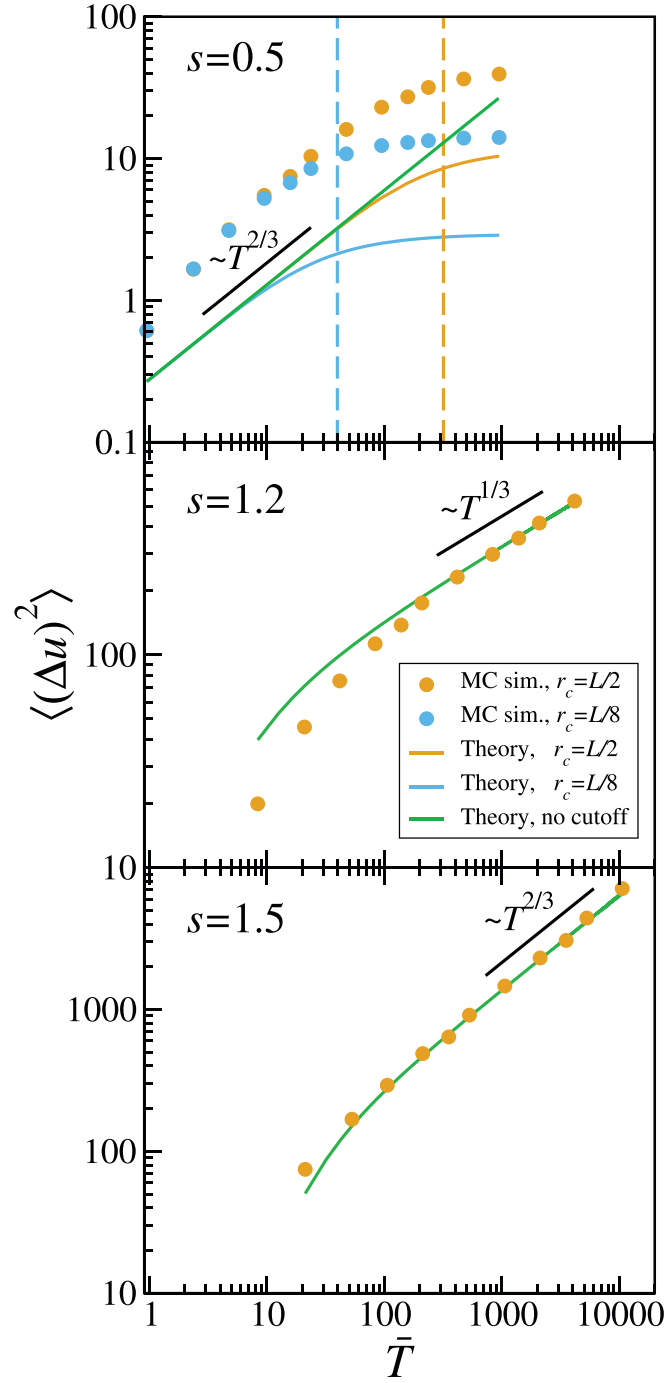


Figure 4. Fluctuations of the potential energy per particle $\langle (\Delta u)^2 \rangle$ as a function of rescaled temperature $\bar{T} = T\rho_0^{-s/2}/v_0$ for $s = 0.5, 1.2, 1.5$, as obtained from MC simulations (circles) and analytical theory (solid lines). The upper panel shows results for two values of the interaction cutoff distance, $r_c = L/2, L/8$, and the analytical result in the absence of cutoff. The vertical dashed lines indicate the temperature above which the screening length λ becomes larger than r_c . In the lower two panels for $s = 1.2, 1.5 > d/2$ the solid curves show analytical results using the fitting parameters $c = 15, 1.5$, respectively. Black lines indicate the power laws predicted in equation (18). The fluctuation axis is rescaled by ρ_0^{-s}/v_0^2 .

fluctuations for $s = 1.2, 1.5 > d/2$ as obtained from theoretical calculations are essentially independent of r_c , implying the dominance of small-wavelength fluctuations. For these two values of $s > d/2$ the simulation data with interaction cutoff show good agreement with the theory without interaction cutoff at relatively high temperatures, where the theory

should hold, once we fit the free parameter c in the relation $K = c/\ell$ (equation (17)). The fitted values, however, differ substantially between the two cases ($c = 15, 1.5$ for $s = 1.2, 1.5$, respectively).

Overall, the simulations confirm the main predictions of the high-temperature theory, namely, the power laws, general

shapes of the curves, and sensitivity to r_c . However, the large quantitative discrepancy for $s = 0.5$ (uppermost panel in figure 4), as well as the very different values of the free parameter c required to fit the curves for $s = 1.2$ and $s = 1.5$ (lower two panels), show that the agreement between simulation and theory is still far from being quantitative.

7. Discussion

Our analytical and numerical results highlight the distinction between repulsive Riesz gases with interaction decay power $s < d/2$, exhibiting hyperuniformity, and ones with $d/2 \leq s < d$, which exhibit hyperuniformity as well as small-scale decorrelation. The entropy of the former is dominated by the cost of suppressed large-scale fluctuations, equation (12). The latter's entropy is dictated by the contribution of small-scale correlations, equations (15) and (18). We have reached these conclusions by noticing the failure of a simple high-temperature theory to yield a physical entropy for the second category. We showed that the theory is regularized by an intrinsic cutoff distance ℓ , akin to the electrostatic Bjerrum length. Our results are practically significant provided that ℓ is larger than the physical lower cutoff distance set by the molecular size. This is the typical case (see examples below). Moreover, as seen in figure 3, the relevant effects set in already at k values much smaller than ℓ^{-1} , which further broadens the range of applicability of our results. At sufficiently high temperature, the regularization of the theory will come from the molecular size a rather than the intrinsic ℓ , changing the dependence of entropy on density and temperature. The modified expressions are obtained from equations (14) and (15) by changing λK to λ/a .

The simple theory gives excellent results for $S(\mathbf{k})$ at high temperature for almost all k values (figure 2). However, it fails at sufficiently high k for *all* temperatures (figure 3). For $s < d/2$ the consequences are unimportant, but for $s \geq d/2$ they are far-reaching. More accurate theories than the simple high-temperature starting point used here were developed for systems with long-range interactions [1–3]. As they did not focus on short-wavelength fluctuations and their contribution to the entropy, they seem to have missed the distinction between the categories of $s < d/2$ and $s \geq d/2$. Such rigorous analyses are clearly warranted, for example, to obtain the crossover occurring around $k \sim \ell^{-1}$ as an analytical result rather than a numerically confirmed Ansatz. This will also make the related free parameter c unnecessary. Better quantitative agreement with simulation results for the energy fluctuations is also desirable. A possible route for such a future extension is to derive a more accurate entropy bound than equation (7), taking into account higher-order correlations.

Notwithstanding, the high-temperature theory seems to become accurate for all temperatures at sufficiently small k , and the agreement with the simulations improves with decreasing s (see figure 2). This success is related to the fact that the theory correctly predicts the hyperuniformity power law at

small k , $S(k) \sim k^\alpha$, as obtained from the general scaling analysis (section 3) and rigorous sum rules [29, 30]. Thus, a similar analysis should be useful for studying large-scale fluctuations (i.e. hyperuniformity) also at low temperature, as long as the system's symmetry is not broken, for example, upon approaching a glass transition. These issues will be the subject of a forthcoming publication.

Interestingly, the large- k features underlying the phenomena that we have presented here are not manifest in the small- r dependence of the pair correlation function $g(\mathbf{r})$. For larger values of s , i.e. stronger repulsion at short distances, $g(r)$ obtained from the simulations is more suppressed at those distances, as expected (not shown here). Yet, there is no qualitative distinction between $s < d/2$ and $s \geq d/2$. The high-temperature $S(\mathbf{k})$ of equation (11) gives a nonphysical $g(\mathbf{r})$ at short distances, $g(r \ll \lambda) \sim r^{-s}$. While this small- r divergence indicates again the inadequacy of equation (11) at large k , it does not distinguish between $s < d/2$ and $s \geq d/2$.

An example of a system which should exhibit the behavior studied here is a dilute cloud of charged particles near a conducting surface. Due to image charges the repulsive pair-potential has $d = 3$ and $s = 2 > d/2$. (Only if two ions happen to be at the same distance from the surface do they interact via a potential with $s = 3$.) For ions of elementary charge e at a typical distance $h \sim 1$ nm from the surface, at room temperature in vacuum or a gas phase, we get $\ell \sim (e^2 h/T)^{1/2} \sim 1\text{--}10$ nm, larger than a typical ion size. Thus, the energy fluctuations of the ion cloud should be dominated by wavelengths of order ℓ and smaller, and obey the scaling given in equation (18), $\langle(\Delta u)^2\rangle \sim \rho_0 T^{1/2}$.

The enhancement of small-scale density fluctuations should hold also for $s > d$, where hyperuniformity does not occur. An experimentally relevant example is a fluid monolayer of dipolar particles aligned perpendicular to a liquid–gas interface. The dipoles interact via a repulsive power-law potential with $d = 2$ and $s = 3$. The interaction is dominated by the gas phase, whose dielectric constant is much smaller than the liquid's. For molecules with a dipole moment $p \sim 1$ D, at room temperature, we get $\ell \sim (p^2/T)^{1/3} \sim 1$ nm, larger than the typical size of a small dipolar molecule. According to equation (18), the energy fluctuations should scale as $\langle(\Delta u)^2\rangle \sim \rho_0 T^{4/3}$. However, the larger the interaction decay power s , the smaller the cutoff distance ℓ . For example, in the case of the Lennard-Jones potential with the conventionally defined parameters ε and σ , we have $\ell \sim (\varepsilon/T)^{1/12} \sigma$. No matter how large the repulsion amplitude ε may be, ℓ is invariably comparable to the molecular size σ , making the results of the present study irrelevant in this case. Indeed, power-law potentials of large s were found to behave similarly to Gaussian potentials despite their very different small- r dependence [46].

To circumvent the issue of system-size effects, and to further highlight the distinction between the two categories, we have used in the simulations a potential that vanishes beyond a cutoff distance r_c of the order of the system size. For $s < d/2$, changing the value of r_c affects the density and energy fluctuations, and the effect is qualitatively captured by the

high-temperature theory (figure 4, uppermost panel). By contrast, the systems with $s \geq d/2$, which are dominated by small-scale fluctuations, are found to be insensitive to the cutoff. Also noteworthy is the effect of r_c on the structure factor $S_c(k)$ (figure 2). For $s < d/2$ the cutoff introduces pronounced oscillations with periodicity $\sim 1/r_c$, whereas for $s > d/2$ the oscillations are negligibly small. In all cases the interaction cutoff makes the small- k dependence of $S_c(k)$ saturate to a constant, removing the hyperuniformity. As $r_c \rightarrow \infty$ the oscillations disappear and the small- k dependence becomes a power law, restoring hyperuniformity.

The distinctive behaviors of systems governed by long-range repulsion with $d/2 \leq s < d$ must affect their dynamics. This calls for separate studies.

Data availability statement

All data that support the findings of this study are included within the article (and any supplementary files).

Acknowledgments

We thank Jürgen Horbach, Yitzhak Rabin and Salvatore Torquato for illuminating discussions. This research has been supported by a joint grant from the Israel Science Foundation and the National Natural Science Foundation of China (ISF-NSFC Grant No. 3159/23). E C O further acknowledges support from RFIS-II Grant by the National Natural Science Foundation of China (Grant No. 12350610238).

ORCID iDs

H Diamant  <https://orcid.org/0000-0003-3858-1114>
E C Oğuz  <https://orcid.org/0000-0001-7648-0010>

References

- [1] Campa A, Dauxois T and Ruffo S 2009 *Phys. Rep.* **480** 57
- [2] Bouchet F, Gupta S and Mukamel D 2010 *Physica A* **389** 4389
- [3] Lewin M 2022 *J. Math. Phys.* **63** 061101
- [4] Brydges D C and Federbush P 1980 *Commun. Math. Phys.* **73** 197
- [5] Alastuey A and Martin P A 1985 *J. Stat. Phys.* **39** 405
- [6] Brydges D C and Martin P A 1999 *J. Stat. Phys.* **96** 1163
- [7] Anteneodo C and Tsallis C 1998 *Phys. Rev. Lett.* **80** 5313
- [8] Martin P A and Yalcin T 1980 *J. Stat. Phys.* **22** 435
- [9] Lebowitz J L 1983 *Phys. Rev. A* **27** 1491
- [10] Jancovici B, Lebowitz J L and Manificat G 1993 *J. Stat. Phys.* **72** 773
- [11] Thomas H, Morfill G E, Demmel V, Goree J, Feuerbacher B and Mohlmann D 1994 *Phys. Rev. Lett.* **73** 652
- [12] Abo-Shaeer J R, Raman C, Vogels J M and Ketterle W 2001 *Science* **292** 476
- [13] Lieb E H and Lebowitz J L 1972 *Adv. Math.* **9** 316
- [14] Gregg J N 1989 *Commun. Math. Phys.* **123** 255
- [15] Barré J, Mukamel D and Ruffo S 2001 *Phys. Rev. Lett.* **87** 030601
- [16] Bouchet F and Barré J 2005 *J. Stat. Phys.* **118** 1073
- [17] Ellis R S, Touchette H and Turkington B 2004 *Phys. A* **335** 518
- [18] Leyvraz F and Ruffo S 2002 *J. Phys. A* **35** 285
- [19] Torquato S and Stillinger F H 2003 *Phys. Rev. E* **68** 041113
- [20] Torquato S 2018 *Phys. Rep.* **745** 1
- [21] Serfaty S 2014 *C. R. Phys.* **15** 539
- [22] Baus M and Hansen J P 1980 *Phys. Rep.* **59** 1
- [23] Forrester P J 1998 *Phys. Rep.* **301** 235
- [24] Hoover W G, Gray S G and Johnson K W 1971 *J. Chem. Phys.* **55** 1128
- [25] Gruber C, Lugrin C and Martin P A 1980 *J. Stat. Phys.* **22** 193
- [26] Pollock E L and Hansen J P 1973 *Phys. Rev. A* **8** 3110
- [27] Travesset A 2014 *J. Chem. Phys.* **141** 164501
- [28] Agrawal R and Kofke D A 1995 *Phys. Rev. Lett.* **74** 122
- [29] Blum L, Gruber C, Lebowitz J L and Martin P 1982 *Phys. Rev. Lett.* **48** 1769
- [30] Martin P A 1988 *Rev. Mod. Phys.* **60** 1075
- [31] Torquato S and Stillinger F H 2006 *Exp. Math.* **15** 307
- [32] Levin Y 2002 *Rep. Prog. Phys.* **65** 1577
- [33] Hansen J P and McDonald I R 2006 *Theory of Simple Liquids* (Elsevier)
- [34] Beck J 1987 *Acta Math.* **159** 1
- [35] Oğuz E C, Socolar J E, Steinhardt P J and Torquato S 2017 *Phys. Rev. B* **95** 054119
- [36] Oğuz E C, Socolar J E S, Steinhardt P J and Torquato S 2019 *Acta Cryst. A* **75** 3–13
- [37] Ariel G and Diamant H 2020 *Phys. Rev. E* **102** 022110
- [38] Sorkin B, Ricouvier J, Diamant H and Ariel G 2023 *Phys. Rev. E* **107** 014138
- [39] Torquato S, Zhang G and Stillinger F H 2015 *Phys. Rev. X* **5** 021020
- [40] Ewald P P 1921 *Ann. Phys.* **64** 253
- [41] Mazars M 2011 *Phys. Rep.* **500** 43
- [42] Hansen J P 1973 *Phys. Rev. A* **8** 3096–109
- [43] Wang H and Torquato S 2024 *J. Chem. Phys.* **160** 044911
- [44] Grigera T S and Parisi G 2001 *Phys. Rev. E* **63** 045102(R)
- [45] Ninarello A, Berthier L and Coslovich D 2017 *Phys. Rev. X* **7** 021039
- [46] Prestipino S, Saija F and Giaquinta P V 2005 *J. Chem. Phys.* **123** 144110